CHAPTER V

SYNTHESIS, GROWTH AND CHARACTERIZATION STUDIES OF SULPHAMIC ACID MIXED PHOSPHORIC ACID (SAPA) UV NLO CRYSTAL

5. 1. Introduction

Global concern has been converged on functional nonlinear optical (NLO) materials which charted the path to harvest energy hugely profitable in laser micromachining, photochemistry, photoemission spectroscopy, lithography, fluorescence detection, surface-enhanced Raman scattering, communication, surgery, atto-second pulse generation etc (Shan 2016). Functional NLO materials are capable of functioning to control and alter electromagnetic radiation in ultraviolet (UV), visible and infrared (IR) spectral regions. Their optical response of crystals is as a function of incident wavelength and frequency and depends on inherent properties like structure, thermal, chemical stabilities and on external fields applied (Sudarsan 2012). Deep UV (DVU) NLO crystals are optically functioning to transmit the light of wavelengths lesser than 200 nm in UV region by cascaded frequency conversion. They have been fabricated by fusing borates, borate-fluorides, carbonate-fluorides and phosphates also with various metal units belonging to alkali, alkaline earth and transition elements. The challenges of decomposing nature of carbonates, hard growth habit and toxicity of beryllium borates, cost effective melt growth techniques were identified. In contrast, phosphate endowed with long chain geometry, good thermal, chemical stabilities, enhanced SHG, easily grown nature circumvent the aforesaid problems (Tran 2016).

Phosphoric acid acts as a good structural modulator in bio-proteins (Rezabkova, 2012) and some amino acids (Ewa 1999) also. Phosphorylation enhances the thermo-chemical stability and electro-optic behaviors of some amino acids (Yokotani, 1989), (Smolin, 2003). Phosphorylated tyrosine crystal plays vital role in celluar communication (Lim 2010, Jin 2012). Phosphates of Magnesium ammonium (Pelvis struvit stones) grow in alkaline urine (Rule 2011). Phosphorylation is an on/off switch for 5-hydroxyconiferaldehyde O-methyl trans ferase activity in poplar monolignol biosynthesis (Wang 2015). Liver kinase was phosphorylated and crystallized (Lu 2017). It regulates its function with sites of DNA damage (Zolner 2011). Phosphoric acid rare earth phosphor materials are suitable for white LED (Huang 2016). Second order NLO crystal $RbTiOPO_4$ (RTP) was grown by top seeded solution growth (TSSG) method. One-dimensional (1D) surface-relief diffraction gratings were formed on the surface of RTP single crystals by ultrafast laser ablation technique (Raj Kumar 2011). A new alkali metal-rare earth polyphosphate $CsSm(PO_3)_4$ has been synthesized by flux method (Hassen 2015). Morpholinium dihydrogen phosphate crystal was grown by slow evaporation method (Rajan Babu 2016). Transparent single crystal of bis guanidinium hydrogen phosphate monohydrate of length 45 mm and diameter 16 mm have been grown from saturated solution of deionized water adopting Sankaranarayanan - Ramasamy method (Jauhar 2016). Large single crystals of optical transparent guanidinium phosphates GuH_2PO_4 and $Gu_2HPO_4{\cdot}H_2O$ are recently grown $\chi^{(3)}$-based nonlinear optical stimulated Raman scattering (Němec 2017). Recently phosphates have been polymerized in $K_4Mg_4(P_2O_7)_3$ and $Rb_4Mg_4(P_2O_7)_3$ and thus SHG response of the phosphates could be enhanced by corner- connected $Mg_4P_6O_{21}$ double layers. Their UV absorption edge was observed at 170 nm, DUV region (Yu 2017).

Thermo-chemical characteristics of phosphoric acid-water binary mixture (Farr 1950) and Phosphoric acid- water - sulfuric acid ternary mixture (Knobeloch 1962) were studied by heating the mixture at various temperatures. By mixing L-arginine and Phosphoric acid, L-arginine phosphate crystal was grown by slow cooling method (Arunmozhi 2004). Single crystals of L-histidine monohydrochloride phosphate (LHP), semi organic crystal were grown by slow evaporation technique (Anuradha 2015). L-thronine phosphate was synthesized by mixing of ortho phosphoric acid with L-threonine in water (Chinnappan 2015). The impact of tartaric acid (Baig 2017a) and salicylic acid (Baig 2017b) on SHG efficiency of KDOP crystal has been studied. Ortho-phosphoric acid mixed 3-aminophenol was crystallized in aqueous solution (Russel Raj, 2012). Polyvinyl alcohols (PVC) and Phosphoric acid were mixed in equimolar ratio in distilled water. Phosphorylated PVC are thermally stable (Somani 2003). PVA was phosphorylated at various pH values and metal ions were incorporated. When pH value is increased, UV absorption was blue shifted with hyper chromic effect (An 1996). Polyvinyl alcohols (PVC) were phosphorylated and their UV absorption behavior was studied. Phosphoric acid was mixed with PVC in different mole ratio. When the concentration was increased in polyvinyl alcohols, UV absorption was blue shifted and optical band cap energy was increased (Saat 2014). Titanium oxide was treated with Phosphoric acid in various molar ratio. It reduced the particle size of TiO (Onoda 2015). Aqueous phosphoric acid solution was mixed with ZnO in equimolar ratio (Onoda 2017). Urea Phosphoric acid crystal was synthesized by mixing urea with phosphoric acid in water and grown by slow evaporation method (Hema 2017). Sulphamic acid dissolved in HCl acts as electrolyte and reduced plutonium to Pu(III) and further mixing of phosphates in the above electrolyte reduced Pu(III) to Pu(IV) (Jackson 1980). The mixture of

phosphoric and sulphuric acids could dissolute the phosphate rocks (Jamialahmadi 1998). The phosphoric acid influences the structural and optical behaviors of many organic and inorganic compounds. This leverages to design Sulphamic acid admixture Phosphoric acid (SAPA) optical functional crystal for desired DUV NLO applications and to characterize its structural, optical, dielectric and mechanical properties.

5. 2. Experimental Techniques: SAPA

5. 2. 1. Reagents

Sulphamic acid (Amino sulphonic acid) (99% pure AR grade) and Phosphoric acid (99.5% pure AR grade) were purchased from E-merck Co Ltd.

5. 2. 2. Synthesis of SAPA

Sulphamic acid was mixed with phosphoric acid in equimolar ratio in a 250 mL borosil glass beaker. This mixture was homogenized in water with the aid of magnetic stirrer at room temperature for 3 hrs. The resultant solution was evaporated at NTP to yield Sulphamic acid mixed phosphoric acid (SAPA) seed crystals.

5. 2. 3. Solubility study

To measure the solubility of SAPA crystal in water, A 250 ml borosil glass beaker filled with 100 ml water was kept in constant temperature bath. An acrylic sheet with a circular hole at the middle covered the top of the beaker. A spindle from an electric motor, placed on the top of the sheet was introduced into the solution. A Teflon paddle attached at the end of the rod stirred the solution. The Crushed powder of SAPA crystal was added in small amounts with water and stirring was continued

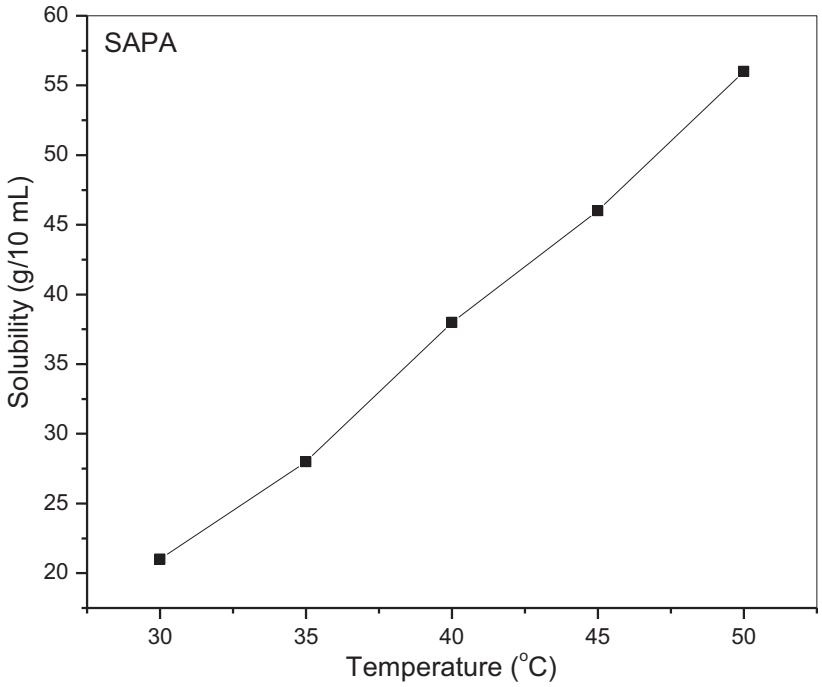

Fig. 5. 1. Solubility curve of SAPA

till the solution attained supersaturation. A 20 ml of the saturated solution was withdrawn by means of a warmed pipette and the same was poured into a clean, dry and weighed Petri dish. The solution was kept in a heating mantle for slow evaporation till the whole of the solution got evaporated and the mass of the SAPA salt in 20 ml of solution was determined by weighing the Petri dish with salt and hence the solubility, i.e quantity of salt in grams dissolved in 100 ml of the solvent was determined. The solubility of SAPA in doubly deionized water was determined for five different temperatures (30, 35, 40, 45 and 50 ^{o}C) by adopting the same procedure. The resulting solubility curve of pure SAPA is shown in Fig. 5.1.

5. 2. 4. Crystal growth technique

SAPA crystals formed in tiny size collected from the admixture solution and dissolved in doubly deionized water with the aid of magnetic stirrer till the solution saturated. The solution was filtered through Whatman filter paper. The filtered solution was collected in a beaker and allowed for slow evaporation by covering with pored acrylic sheet at top of the beaker. After 30-35 days, all solvent dried and SAPA crystal was grown at the bottom of the beaker. Fig. 5. 2 displays the SAPA crystal grown with a size of 38 x 28 x 5 mm^3 harvested from the aqueous solution. This facile route line materialized a UV transmittable NLO crystal Sulphamic acid mixed Phosphoric acid (SAPA) grown in aqueous solution.

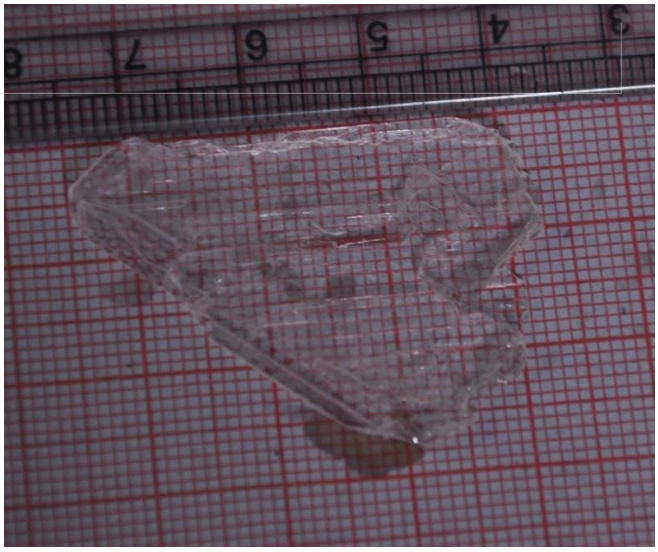

Fig. 5. 2. Photograph of as grown SAPA UV NLO Crystal

5. 3. RESULTS AND DISCUSSION

SAPA crystal was subjected to the following studies:

i. Single crystal X-ray Diffraction analysis (XRD) for measuring unit cell parameters.

ii. X-ray Powder Diffraction analysis (XRPD) to identify the crystalline phase with crystallinity.

iii. FTIR analysis to trace out the spectral map and confirm the various functional groups present in SAPA molecule.

iv. UV-Vis-NIR analysis to study the optical absorption behavior of SAPA crystal and to calculate its optical band gap energy.

v. Dielectric measurement technique to investigate the dielectric response of SAPA for various frequency range

vi. Photoconductivity study to measure the photo responsiveness of the crystal

vii. NLO test to check the non-linear response of the crystal to the incident coherent light

viii. The phase matching between illuminated laser beams and second harmonic waves generated from SAPA crystalline medium was identified.

ix. Vicker's microhardness test to study the harness of the SAPA crystal

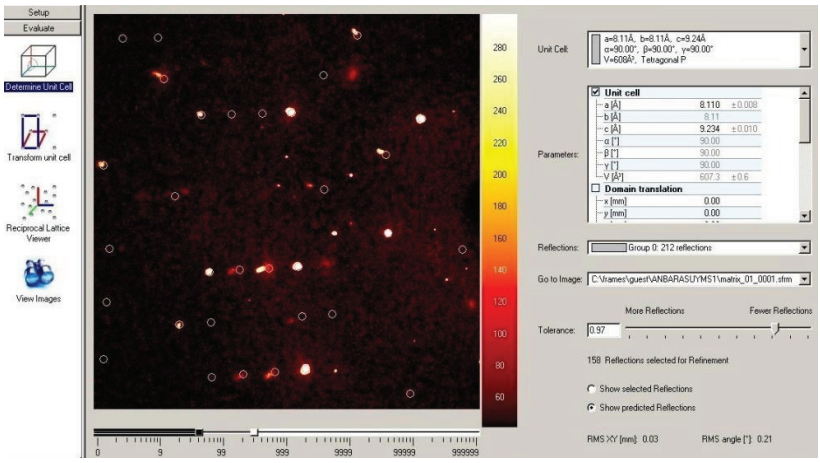

Fig. 5. 3. Single crystal XRD image of SAPA UV NLO Crystal

5. 3. 1 Single Crystal X-Ray Diffraction analysis

Bruker AXS Kappa Apex II CCD Diffractometer equipped with graphite monochromated Mo (Kα) (λ = 0.71073 Å) radiation diagnosed the crystal structure of SAPA. A suitable size SAPA crystal fixed at the tip of the glass fiber using cyano acrylite adhesive was mounted on the goniometer head with the aid of video microscope and optically centered at the goniometer axes. The automatic cell determination routine, with 36 frames at three different orientations of the detector was employed to collect reflections for unit cell determination. Indexing and unit cell dimensions were found out using Apex2 software by difference vector method.

Fig. 5. 3 screened the diagnostic report of SAPA structure which reveals that SAPA crystallized in Tetragonal P crystal system with unit cell parameters of a = b = 8.11 Å, c = 9.24 Å and α=β=γ =90°, and V = 608 $Å^3$. SAPA molecule ordered in tetragonal P crystal system. Pure sulphamic acid crystallized in orthorhombic system (Kanda 1951), (Valluvan 2006). The modulator phosphoric acid (Ewa 1999) distorted the structure of sulphamic acid from orthorhombic by equalizing two lattice parameters a and b.

5. 3. 2. Powder X-Ray Diffraction Analysis

Powder X-ray diffraction (PXRD) patterns were acquired with a XPERT-PRO powder diffractometer. Ground sample was placed on a quartz sample holder and was mounted on the diffractometer. Cu Kα radiation of wavelength λ = 1.5418 Å illuminate the sample and the resultant diffracted beams were collected over the range of 10–80^o with a scan speed of 0.2^o/s. Fig. 5. 4 displays the powder XRD pattern of SAPA. The pure crystalline phases were identified their corresponding *hkl* plane values were manually indexed (Hesse 1948).

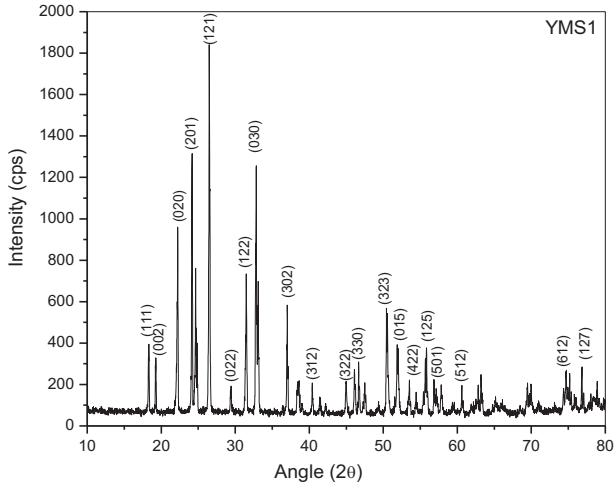

Fig. 5. 4. Powder XRD pattern of SAPA UV NLO Crystal

It was observed that (121) plane highly diffracted at the Bragg's angle (2θ) of 26.29° with FWHM of 0.0502°. Other major peaks were also observed due to the planes (201) and (030) diffracted at 24.64° and 33.10° respectively. Phosphoric acid reduced the particle size of TiO crystal and altar the peak intensity (Onoda 2015). The peaks observed at various Bragg's angles with different intensity reveal the SAPA crystal is deviated to tetragonal from orthogonal of pure sulphamic acid crystal (Valluvan 2006), (Ramesh Babu 2010), (Thaila 2011). This PXRD pattern confirms the existence of mixed crystal system of and sulphamic acid and phosphoric acid.

5. 3. 3. FTIR analysis

FTIR spectrometer (Bruker model IFS 66 V) recorded the FTIR spectra of crushed SAPA crystal powder embedded in KBr matrices in the range 400-4000 cm^{-1}. Fig. 5. 5 displays the FTIR spectrum which draws the map of the characteristic vibrations of the functional groups associated with sulphamic acid influenced by phosphoric acid. The phosphate ion $[PO_4]^{3-}$ exhibits in SAPA is confirmed by its stretching at 1069 cm^{-1}. The P-OH stretching vibration is identified by peaks at 2349, 1004 cm^{-1}. P=O makes resonance broadly around 1275, cm^{-1}. The asymmetric stretching of O-P-O is identified by the peak around 1275 while asymmetric stretching of O-P-O makes peaks at 1004 cm^{-1}. P-OH stretching was traced out at 1069 cm^{-1}. NH_3^+ group stretched symmetrically and asymmetrically at 1539 cm^{-1} and 1448 cm^{-1} respectively. The peaks at 3147 cm^{-1} and 691 cm^{-1} are due to N-H stretching and N-S stretching respectively. N-H bending resonates at 1571cm^{-1}. The peak at 2873 cm^{-1} is assigned to N-H…O vibration. S=O stretching was observed at 1183 cm^{-1}. The peak at 1571cm^{-1} is attributed to SO_2 attached with amino functional group. The shift in standard absorption peaks of all functional moieties are reasoned with the mixed state of sulphamic acid and phosphorus acid in SAPA molecule.

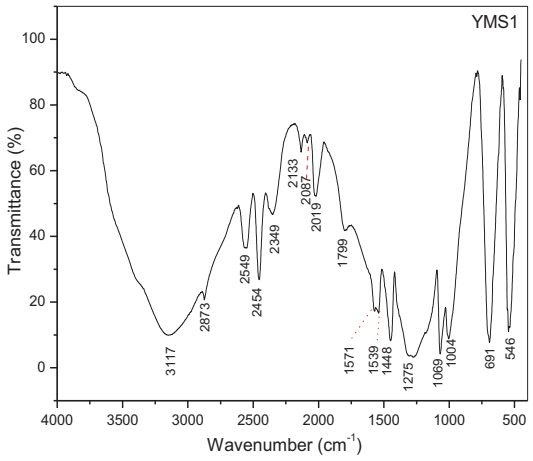

Fig. 5. 5. FTIR spectrum of SAPA UV NLO Crystal

5. 3. 4. Optical Absorption study

Optical transmittance spectrum was recorded using Varian Cary 5E-UV-vis-NIR spectrometer in the wavelength region of 200 – 800 nm. Fig. 5. 6. depicts the optical transmittance spectrum showing SAPA emanate UV radiation from 200 nm with short cut-off value of 222 nm. Wavelength increases from 200 nm to 210 nm, transmittance percentage exponentially increases from 73to 95%. But UV transparency for urea phosphoric acid is 55% (Hema 2017). Various phosphoric acid containing crystal transmits UV light with long cut-off values. For Morpholinium dihydrogen phosphate UV cut-off value was observed at 289 nm (Rajan Babu 2016), for pphosphoric acid mixed 3-aminophenol at 306 nm (Russel Raj 2012), for 0.5 mol% phosphoric acid added PVC at 270 nm (Saat 2014), for Cu(II) ion mixed Phosphorylated PVC prepared in pH >7.0 at 218 nm (An 1996), for Fe(III) – phosphoric acid at 290.5 nm. (Jin 2014) and for urea phosphoric acid at 270 nm (Hema 2017),

The optical absorption coefficient (α) was calculated from the transmittance using the relation

$$\alpha = (2.3036/d) \log(1/T) \qquad \text{-------- (1)}$$

where d is the thickness of the crystal and T is the transmittance.

The optical band gap E_g is calculated from the Tauc's expression,

$$(\alpha h\nu)^n = A(h\nu - E_g) \qquad \text{--------- (2)}$$

where α is the absorption coefficient, A is disorder parameter. E_g is calculated from the plot $(\alpha h\nu)^n$ versus hν. For the direct band gap energy n = 2 and for the indirect bandgap energy n= (1/2).

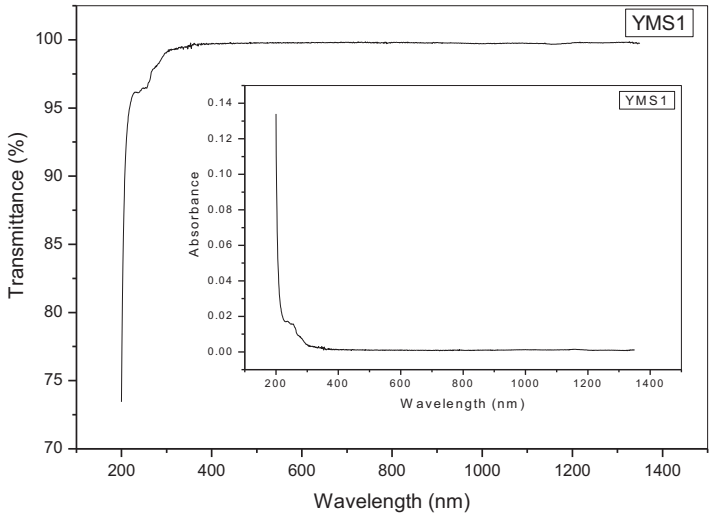

Fig. 5. 6. Optical transmittance of SAPA UV NLO Crystal. The insert is the absorbance spectrum

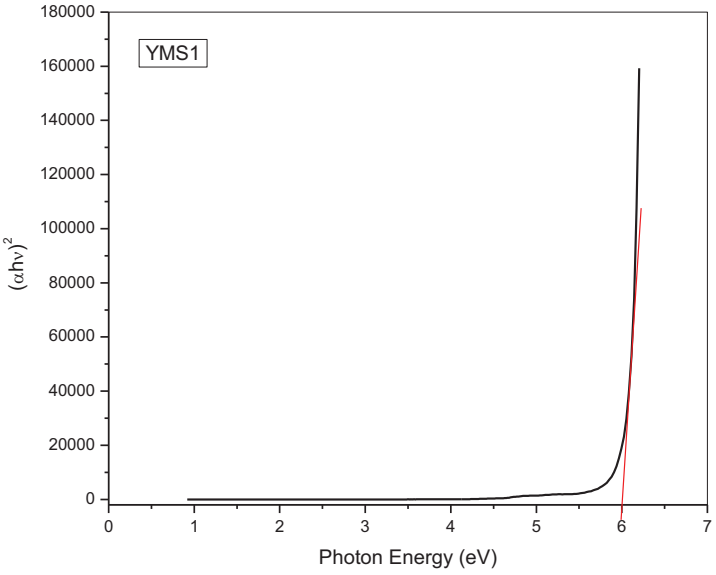

Fig. 5. 7. Tauc's Plot for direct optical band gap energy of SAPA UV NLO Crystal

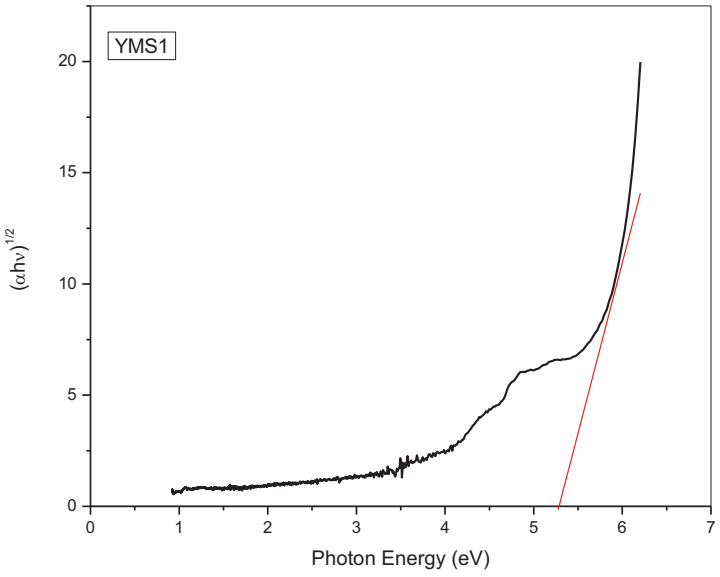

Fig. 5. 8. Tauc's Plot for indirect optical band gap energy of SAPA UV NLO Crystal

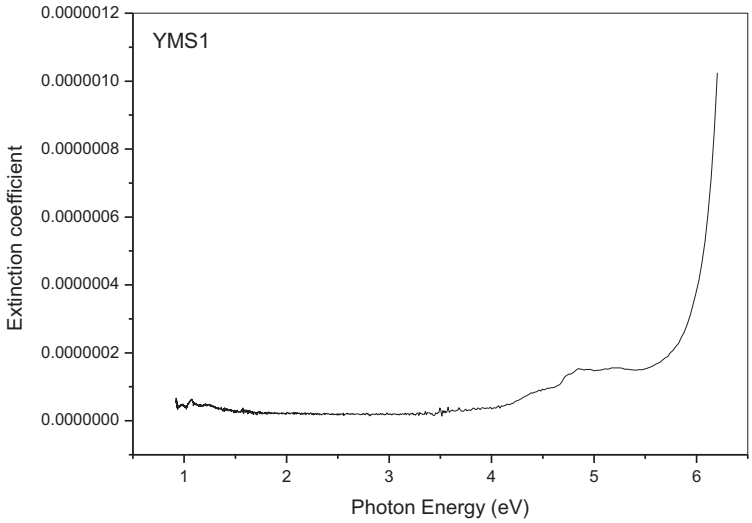

Fig. 5. 9. Plot of Extinction coefficient of SAPA UV NLO Crystal

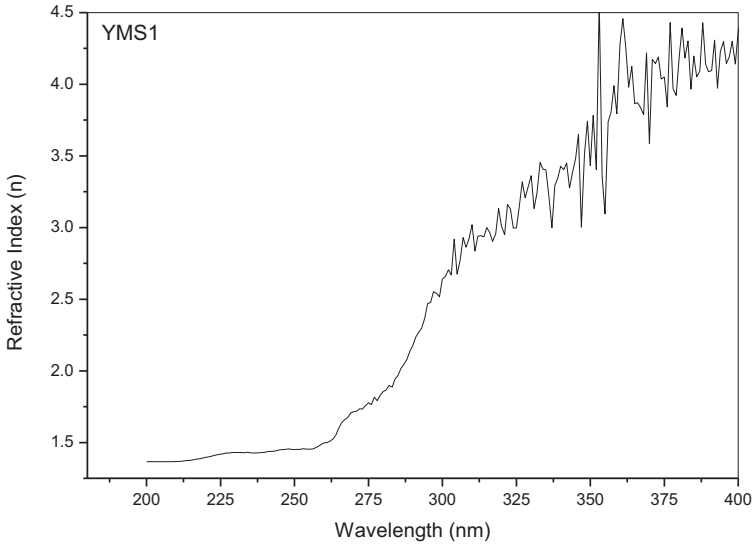

Fig. 5. 10. Plot of Refractive Index of SAPA UV NLO Crystal

Fig. 5. 7 & Fig. 5. 8. show the plot for direct transition and indirect transition respectively. From the graph it was observed that the direct band gap energy $E_{g(direct)}$ = 6.02 eV and indirect band gap energy $E_{g(indirect)}$ = 5.27 eV. The optical band gap energy for Morpholinium dihydrogen phosphate was calculated as 4.03 eV. (Rajan Babu 2016), for Ortho-phosphoric acid mixed 3-aminophenol - 4.05 eV (Russel Raj, 2012), for 0.5 mol% phosphoric added PVC 5.83 eV (Saat 2014) and for urea phosphoric closer to 4 eV (Hema 2017). Higher optical band gap energy value enhances the SAPA crystal for laser generation and other NLO applications.

The extinction coefficient of SAPA crystal was plotted against the energy as shown in Fig. 5. 9 and the refractive index was against wavelength as shown in Fig. 5. 10. SAPA exhibits low extinction coefficient and low refractive indices in UV region. Wider UV transmittance window with low refractive index, low extinction coefficient and high optical band cap energy make SAPA suitable for various optical applications.

5. 3. 5. Dielectric studies

Dielectric behavior of SAPA was studied in the frequency range of 50 Hz to 5 MHz using Hioki 3532-50 LCR Hitester at various temperatures (40, 50, 60 ,70 ^{o}C). The plots of dielectric constant (ε_r) and dielectric loss (D) were drawn against frequency (log f) for different temperatures as shown in Fig. 5. 11 & Fig. 5. 12 respectively. SAPA molecules polarized effectively when local electric field of low frequency induced them, due to the sum of space charge, dipolar, ionic and electronic polarizability. As the frequency of electric field increases, charge, dipolar, ionic polarizabity became ineffective except electronic polarizability and the relative permittivity of SAPA decreases as well as dielectric loss.

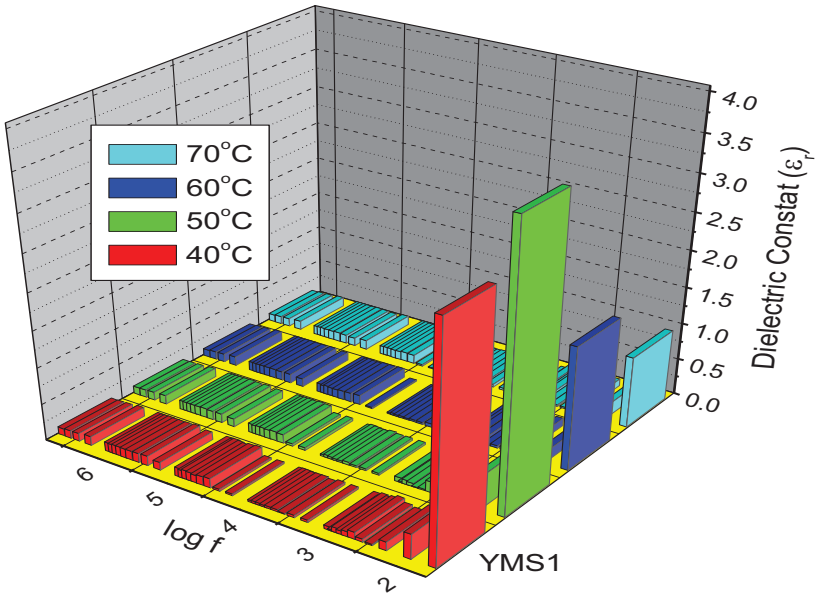

Fig. 5. 11. Plot of Dielectric constant of SAPA UV NLO Crystal

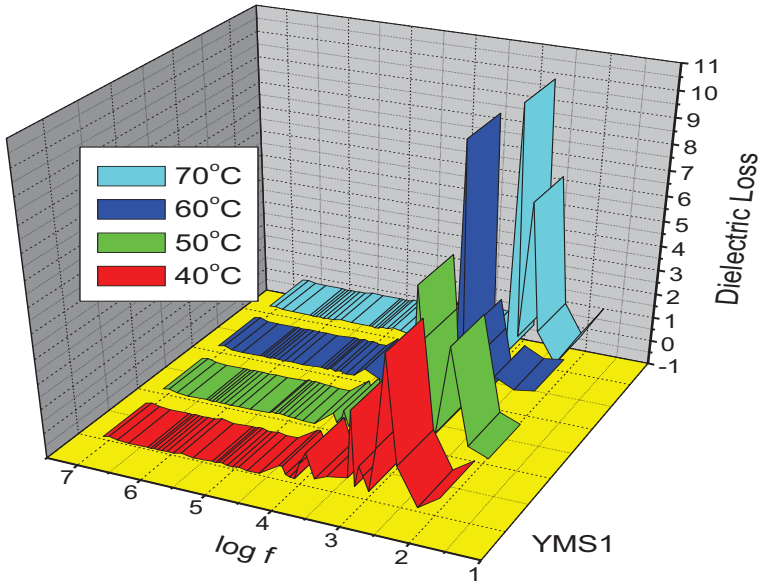

Fig. 5. 12. Plot of Dielectric loss of SAPA UV NLO Crystal

This normal dielectric sense of SAPA discloses its charge transport mechanism and electric field distribution at all temperatures. The maximum values of dielectric constant of SAPA at 50 Hz were calculated as 3.12, 3.76, 1.67 and 0.97 at 40, 50, 60 and 70 ^{o}C respectively.

5. 3. 6. Photoconductivity study

Keithley 485 pico ammeter measured the photoconductivity of SAPA samples. Initially, the sample was kept away from any other radiations. The crystal sample was connected in series to a DC power supply and pico ammeter. Silver paint was coated on sample to make the electrical contacts. The radiation from a halogen lamp containing iodine vapour was exposed on the sample by focusing a spot of light on the sample with the help of a convex lens. The photocurrent (I_p) was calculated. Initially the applied voltage was increased from 0 to 100 V in steps of 20 V and the corresponding dark currents were measured. Fig. 5. 13 displays the plot of variation of both the dark current and photo current of the sample against the applied voltage. Both the dark and photocurrent were seen to increase linearly with the applied field. For the same applied field, the photo current is less than the dark current which reveals the negative photo conducting behaviour of SAPA crystal. Urea Phosphoric acid also shows negative photoconductivity (Hema 2017).

5. 3. 7. NLO Test

In Kurtz-Perry powder test, Nd: YAG laser having fundamental radiation of 1064 nm with an input power 0.68 J as the optical source and illuminated on to the powdered sample of SAPA through a visible blocking filter. a monochromator collected the 532 nm radiation after spreading the 1064 nm pump beam with an infrared blocking filter. SAPA emanated second harmonics of primary Nd:YAG laser.

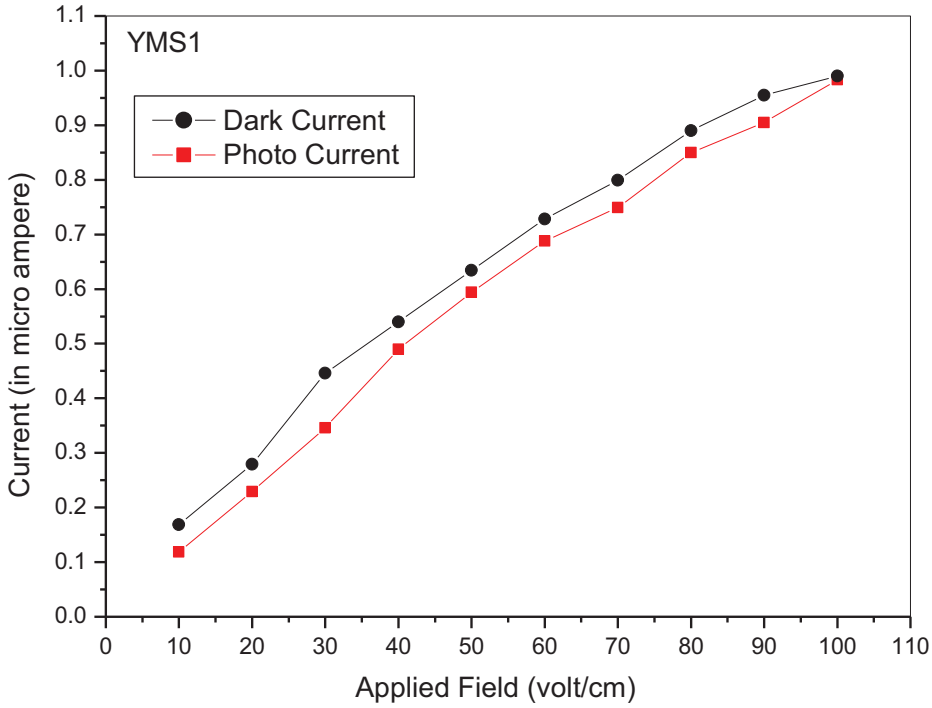

Fig. 5. 13. Photoconductivity of SAPA UV NLO Crystal

Powder SHG efficiency was measured by a photomultiplier tube. A sample of KDP was used as a reference material for the present measurement. It is found that the SAPA single crystal has an efficiency of 0.59 times that of KDP.

5. 3. 8. Phase Matching analysis

SAPA crystalline sample was ground and sieved into distinct particle sizes in the range of less than 106, 106-125, 125-150 and above 150 μm. KDP crystal was also sieved into the particle dimension of SAPA. Q-switched Nd:YAG infrared laser pulses irradiated on the sieves. SHG efficiency depends on the particle size and varies with size of sieves. SHG output was measured and plotted for various particle size. SHG intensities increased with increasing particle size upto 150 μm as shown in Fig. 5. 14 vowing the phase matching behavior of SAPA. It is a promising phase matchable NLO crystal for LASER generation.

5. 3. 9. Microhardness study

Leitz Wietzlar Vickers Microhardness tester measured the hardness parameters of single crystal of SAPA at room temperature. Flat shape crystal was fitted with a Vickers diamond pyramidal indenter light microscope. The static indentations were made at room temperature with a constant indentation time of 15 seconds for all indentation. The indenter marked on the crystal surfaces by varying the load from 20 to 100 g.

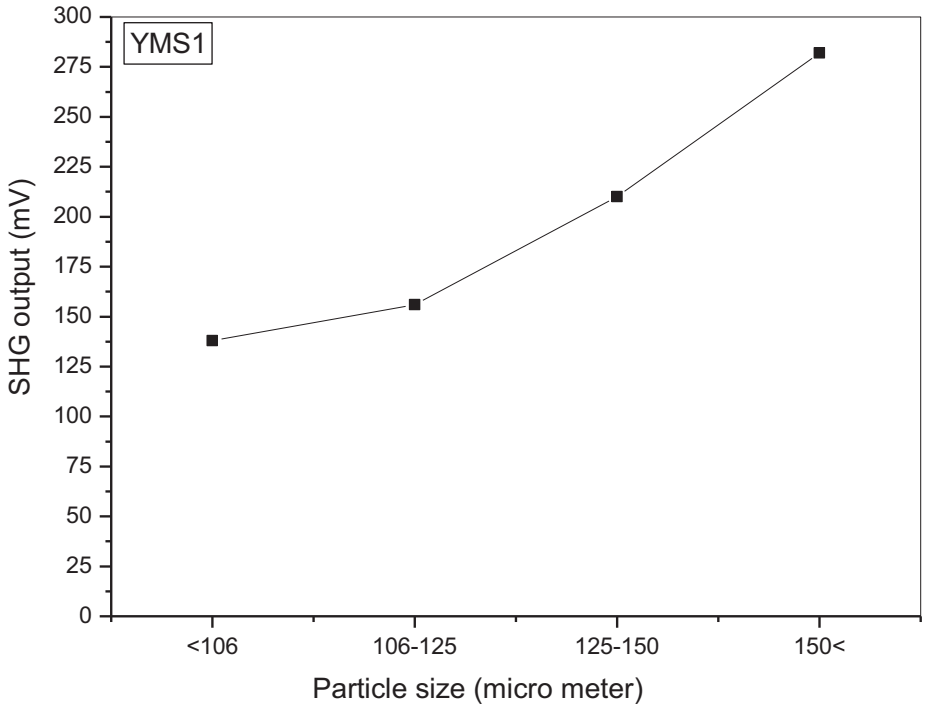

Fig. 5. 14. Phasematching curve of SAPA UV NLO Crystal

The Vickers microhardness number H_v of the crystal was calculated using the relation

$$H_v = 1.8544\ P/d^2\ Kg\ mm^{-2} \quad \text{---------- (3)}$$

where P is the applied load and d is the average diagonal length of the indented impression in mm. Vickers microhardness profile as a function of load is shown in Fig. 5. 15. (a)

By using Meyer's law, the load P is related with the indentation size as

$$P = k_1 d^n \quad \text{---------- (4)}$$

Mayer constant (k_1) and work hardening coefficient (n) are the constants for a particular sample. The work hardening coefficient n is calculated from the slope of the curve drawn by plotting log (P) against log (d) as shown in Fig. 5. 15 (b)

The value of k_1 was measured from the derivative of the curve drawn by plotting P against d^n as shown in Fig. 5. 15 (c). The value of n is found to be 2.45.

If n is greater than 2, the microhardness number H_v increases with increasing load (Onitsch 1947, Hanneman 1941), The work hardening coefficient value of SAPA proves that SAPA is a soft material.

The degree of dislocation density of the material is related with load P and indentation d through Kick's law given by

$$P = k_2(d+x)^2 \quad \text{---------- (5)}$$

By simplifying Eqn. (4) and (5) we get

$$d^{n/2} = (k_2/k_1)^{1/2}\ d + (k_2/k_1)\ x \quad \text{---------- (6)}$$

$d^{n/2}$ is plotted against d as shown in Fig. 5.15(d) and the slope of the straight line yields $(k_2/k_1)^{1/2}$ and the intercept is a degree of x.

The yield strength of the material is given by

$$\sigma_v = (H_v/2.9)\{[1-(2-n)]\ x\ [(12.5)(2-n)/(1-(2-n))]^{2-n}\} \quad \text{---------- (7)}$$

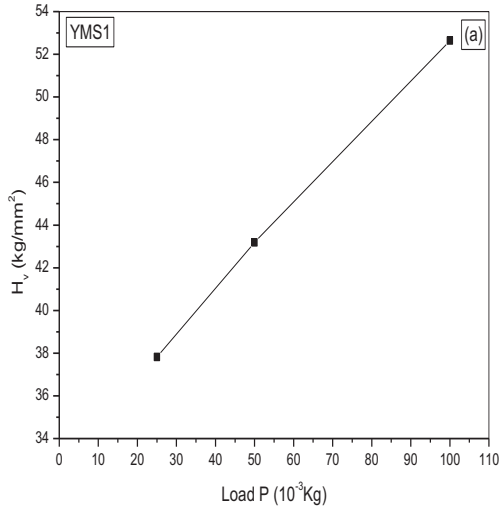

(a) Variation of hardness with load

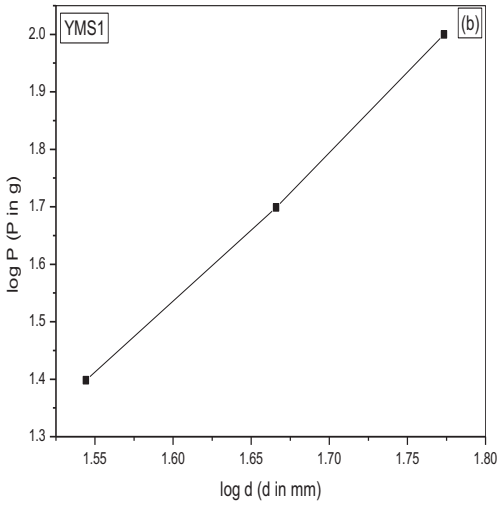

(b) Plot of log P Vs log d

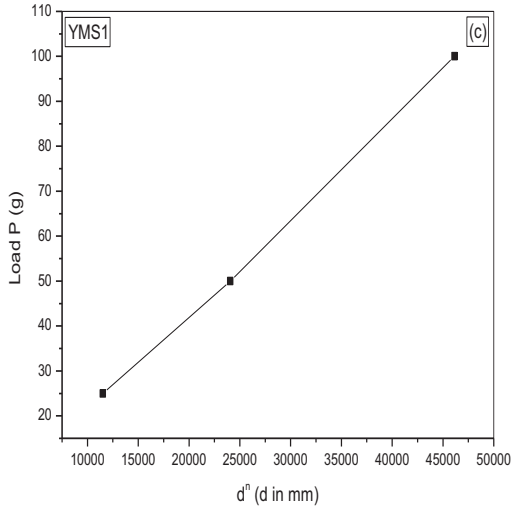

(c) Plot of d^n Vs P

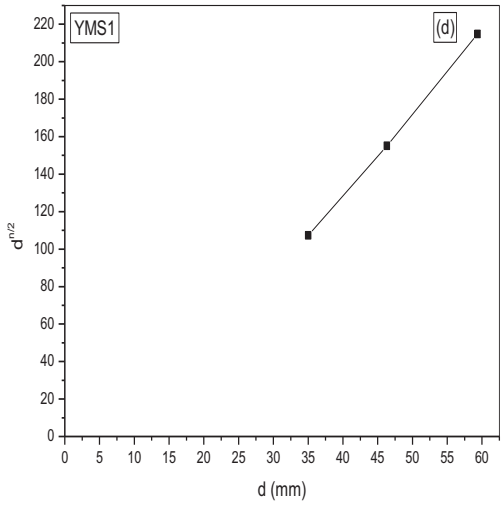

(d) Plot of log d Vs $d^{n/2}$

Fig. 5. 15. Microhardness measurements of SAPA single crystal. (a) Variation of harness with load, (b) Plot of log P versus log d, (c) Plot of d^n versus P, (d) Plot of d versus $d^{n/2}$.

Table 5. 1. Hardness Parameters of SAPA UV NLO Crystal

Hardness Parameters	Calculated Value
N	2.63
k_1	2.12 (10^{-3} Kg)
k_2	41.04 (10^{-3} Kg)
X	10 (μm)
σ_v	9.26 (MPa)

From the graphs, the constants k_1, k_2 and x are evaluated and the yield strength (σ_v) of SAPA is computed. Hardness parameters of SAPA crystal are tabulated in Table 5.1. As the work hardening coefficient value of SAPA is n=2.45, it suggests that SAPA is a soft material. The incorporation of phosphoric acid supported the soft growth habit and made it feasible to process. Phosphoric acid treated ZnO was smoothened (Onoda 2017).

5. 4. Conclusion

Sulphamic acid mixed Phosphoric acid crystal (SAPA) was grown in aqueous solution by slow evaporation technique. The Phosphorylation distorted sulphamic acid to be crystallized in Tetragonal crystal system. The functional groups of sulphamic acid and phosphoric acid were confirmed by FTIR spectroscopy technique. Wider UV transmittance window starts with short cut-off at 222 nm. The optical band gap energy of SAPA is 6.02 eV. UV light could travel through SAPA crystal faster. The dielectric sense of SAPA molecules was confirmed. SAPA exhibits negative photo conducting behavior. It is a phase matchable second order NLO crystal. Its SHG efficiency was calculated as 0. 59 times that of KDP. Soft crystal growth habit made it feasible to process. SAPA is a UV transmittable crystal suitable for various energy harvesting processes.